島根大学学術情報リポジトリ
SWAN
Shimane University Web Archives of kNowledge

Title

Negative Hall Factor of Acceptor Impurity Hopping Conduction in p-Type 4H-SiC

Author(s)

Yasutomo Kajikawa

Journal

Journal of Electronic Materials volume 50, pages1247–1259 (2021)

Published

04 January 2021

URL

https://link.springer.com/article/10.1007/s11664-020-08639-0

この論文は出版社版でありません。
引用の際には出版社版をご確認のうえご利用ください。

Negative Hall factor of acceptor impurity hopping conduction in *p*-type 4H-SiC

Yasutomo Kajikawa

Interdisciplinary Faculty of Science and Engineering, Shimane University, Matsue 690-8504, Japan

e-mail kajikawa@riko.shimane-u.ac.jp, Phone: +81 852 32 8903, Fax: +81 852 32 8903

The experimental data of the temperature-dependent Hall-effect measurements on Al-doped p-type 4H-SiC samples, which exhibit the anomalous sign reversal of the Hall coefficient to negative at low temperatures, have been analyzed on the basis of an impurity hopping conduction model previously proposed. According to the small polaron theory for the non-adiabatic case, the activation energy E_3 for the drift mobility of nearest-neighbor hopping has been deduced with taking into account the temperature dependence of the pre-exponential factor. Existing models on the sign of the Hall coefficient have been critically examined. It is shown that the anomalous sign reversal of the Hall coefficient can be well explained by assuming the hopping Hall factor in the form of $A_{H3} = (k_B T/J_3)\exp(K_H E_3/k_B T)$ with the negative sign of J_3.

Keywords Silicon carbide; Hall effect; impurity band; hopping conduction

INTRODUCTION

It has been known that heavy doping reduces the thermal activation energy of dopants in semiconductors and leads to impurity hopping conduction. However, the Hall effect for impurity hopping conduction is not well understood yet. Although several theories have been developed for the hopping Hall effect, the comparison of the theories with the experimental results is still not enough. Low-temperature anomalies in the conductivity and the Hall coefficient due to impurity hopping conduction were first discovered by Buch and Labhart [1] in SiC before they were discovered by Hung and Gliessman [2] in Ge. Thereafter, huge numbers of studies had been devoted for impurity hopping conduction in Ge, but only several studies [3-8] had been devoted for that in SiC in the 20th century.

Impurity hopping conduction due to Al acceptors in p-type 4H-SiC has been reported since 1999 in Refs. [9-18]. Among these reports, the anomalous sign reversal of the Hall coefficient has been reported by Tone and Zhao [9], then by Contreras et al. [13] and Matsuura et al. [18]. The similar anomaloussign reversal of the Hall coefficient has also been observed for Al-doped p-type 6H-SiC [19] as well as other various p-type materials such as Ge [20], Mn-doped InSb [21-26], Mg-doped InP [27, 28], Mn-doped InP [29], Mg-doped GaN [30], Gd-doped $LaCaMnO_3$ [31], and Be-doped GaAs/AlGaAs quantum wells [32]. Among these experimental data, the sign reversal of the Hall coefficient has been analyzed in the previous studies of the author for Mg-doped GaN [33], Mn-doped InSb [34], and Mg-dopedInP [35]. In the present study, the sign reversal of the Hall coefficient observed for Al-doped p-type 4H-SiC by Contreras et al. [13], Matsuura et al.[18], and by Tone and Zhao [9] is analyzed within a model similar to that in the previous studies of the author on the above-mentioned III-V materials [33-35].

In the following, the analysis model is described in Sec. 2.We then describe in Sec. 3 the results of simultaneous fits to the experimental data of the conductivity σ and the Hall coefficient R_H on the Al-doped p-type 4H-SiCsamples reported by Contreras et al. [13], Matsuura et al. [18], and Tone and Zhao [9]. Parameters related to impurities are deduced there. Then, the relations among the deduced parameters are discussed in Sec. 4. The summary is given in Sec. 5.

ANALYSIS MODEL

For SiC, Al is the preferred acceptor species to obtain a p-type conductivity because of its lower ionization energy compared to other acceptors. Al doping introduces two acceptor levels in SiC. In highly doped materials, however, it has been shown in Refs. [13, 36] that the deeper acceptor level is negligible in the temperature dependence of the Hall carrier concentration up to 700 K. Therefore, only

a shallow acceptor level with a compensation donor level was assumed in the present study. The acceptor degeneracy factor g_A was assumed to be 4.

The analysis model used in present study is almost the same as that has been used in the analyses of the transport data on p-type III-V materials in the previous studies [33-35].When taking into account impurity hopping conduction besides free-hole conduction, the total conductivity $\sigma$is represented by $\sigma = \sigma_v + \sigma_{ib}$, where σ_v and σ_{Ib} denote the free-hole conductivity and the impurity hopping conductivity, respectively. The respective conductivities are calculated as $\sigma_v = en_v\mu_v$ and $\sigma_{ib} = en_{ib}\mu_{ib}$, where e is the elemental charge, n_v is the free-hole concentration while n_{ib} is the effective concentration of carriers hopping in the impurity band; μ_v and μ_{ib} denote drift mobilities for free-hole conduction and impurity conduction, respectively. For p-type semiconductors, $n_{ib} = N_A^- N_A^0 / N_A$, where N_A^- and N_A^0 denote the concentrations of ionized and neutral acceptors, respectively, while N_A denotes the total concentration of the shallow acceptors [37, 38]. The concentrations of ionized and neutral acceptors are calculated as $N_A^- = N_A f_A$ and $N_A^0 = N_A(1 - f_A)$, respectively, where $f_A(E) = \left[1 + g_A \exp\left(\frac{E_F + E}{k_B T}\right)\right]^{-1}$ denotes the occupation probability of an acceptor level by an electron withE_F, k_B, and T being the Fermi level, the Boltzmann constant, and the absolute temperature,respectively. At low temperatures, n_{ib} is approximated as $n_{ib} \approx N_D(N_A - N_D)/N_A$, where N_D denotes the concentration of compensating donors.

The total Hall coefficient is represented by$R_H = (\sigma_v/\sigma)^2 R_{Hv} + (\sigma_{ib}/\sigma)^2 R_{Hib}$. The Hall coefficient for free-hole conduction in the valence band is defined as $R_{Hv} = A_{Hv}/(en_v)$, where A_{Hv} is the Hall factor of free holes in the valence band, while that for the impurity hopping conduction is defined as R_{Hib} =

$A_{Hib}/(en_{ib})$, where A_{Hib} is the Hall factor for the impurity hopping conduction. Then, the Hall mobility is calculated as $\mu_H = |R_H|\sigma$.

We assume here the nearest neighbour hopping (NNH) as the hopping mechanism in the acceptor impurity band and assume the form of [39, 40]

$$\mu_{ib} = \mu_{ib0}(E_3 / k_B T)^s \exp[-(E_3/k_B T)], \quad (1)$$

where μ_{ib0} and $E_3 = k_B T_{03}$ are adjustable temperature-independent parameters.

The physical picture for the NNH process is based on occasional dynamic fluctuations of the lattice which at a given moment may produce equal distortions at the occupied and a neighbouring site. The electric energy of the two adjacent sites will become momentarily equal and the carrier will have a certain probability of tunnelling. The momentary occurrence of equal energy was called a "coincidence event" by Holstein [41, 42]. The transition probability during a coincidence event was studied in two limiting cases, called the adiabatic and non-adiabatic regimes. In adiabatic regime the carrier can follow the motion of the lattice and will possess a high probability of hopping to the adjacent site during a coincidence event. In non-adiabatic regime the carrier cannot follow the lattice vibration and the time required for a carrier to hop is large compared to the duration of a coincidence event. In this case many coincidence events will occur before the carrier hops to the neighboring site.

Shklovskii and Efros [43] theoretically derived that $s = 1$ (Eq. (9.4.3) in Ref. [43]). Note, however, that this stands only for the adiabatic case. In case of the non-adiabatic case, it has been shown $s = 3/2$ [39, 40] (Eq. (3.2.21) in Ref. [39]).

Mansfield [44] has pointed out that, for deducing the hopping activation energy correctly, it is necessary to include properly the temperature dependence of the pre-exponential factor σ_{ib0}. When assuming a form of $\sigma_{ib0} \propto (E_3/k_BT)^s = (T_{03}/T)^s$, the slope of the Arrhenius plot of σ_{ib} can be written as

$d(\ln\sigma_{ib})/d(1/T) = -T_{03} + sT$. Namely, the slope of the Arrhenius plot of σ_{ib} will decrease with temperature. The temperature dependence of the pre-exponential factor can be neglected only if $T << T_{03}$. As has been pointed out by Mansfield [44], one should have to plot $\ln(\sigma T^{s})$ as a function of reciprocal temperature, if one wants to obtain the correct value of T_{03}.

For their p-type samples of Al-doped and Al-N codoped 4H-SiC, Matsuura et al. [15] plotted the resistivity as a function of the reciprocal temperature. In the Arrhenius plots of the resistivity, they found that, for the samples with the Al concentrations between 1×10^{19} cm^{-3} and 4×10^{19} cm^{-3}, another conduction region appears between the free-hole conduction and the NNH regions. As the conduction mechanism for this region, Matsuura et al. [15] proposed two models. They referred the two model as the dopant-concentration inhomogeneity model and the emission-hopping model. In the former model, the regions with two different values of the Al concentration are assumed in a sample. The latter model resembles the model that Poklonski et al. [45, 46] called jumping conduction. In both the models, capture of free holes from the valence band by acceptors occurs so that a hole travels through the free-hole and NNH conductions alternatively.

Figure 1 shows the Arrhenius plots of the experimental results for two samples of p-type 4H-SiC reported by Matsuura et al. [15]:Closed squares and triangles respectively represent the plots of σ for the Al-doped sample with the Al concentration of 2.4×10^{19} cm^{-3} and for the Al-N codoped sample with the concentrations of Al and N of 1.4×10^{19} cm^{-3} and 7.0×10^{18} cm^{-3}. It seems from these two Arrhenius plots of σthat another conduction region might appear between the free-hole conduction and the NNH regions. On the other hand, open squares and triangles in Fig. 1respectively represent the plots of $\sigma T^{3/2}$ for the former and the latter samples. It can be seen from these plots that there is no need to assume another conduction mechanism between the free-hole conduction and the NNH regions if

assuming the pre-exponential factor σ_{ib0}having the temperature dependence in the form of $(T_{03}/T)^s$ with s = 3/2. Similarly, it has been shown in the previous studies of the author on p-type GaAs [47] and InP [35] that the Arrhenius plots of $\sigma T^{3/2}$ in the NNH conduction region result in straight lines whereas those of σ exhibit the saturated behaviour with increasing temperature. Then, the temperature dependence of the pre-exponential factor with s = 3/2 was adopted for the analyses in these previous studies. In the present analysis, the value of s = 3/2 is also adopted as in the previous studies of the author [33-35, 47]. Note, however, that there is a possibility that s decreases from 3/2 to less than 3/4 as the major impurity concentration approaches to the critical concentration for the onset of the metal-insulator (MI) transition, as shown in Ref. [48]. Actually, Matsuura et al. [15] found that the data in the Arrhenius plots for the samples with the Al concentrations between 4.9 × 10^{19} cm^{-3} and 1.8 × 10^{20} cm^{-3}can be approximated by two straight lines without taking into the temperature dependence of the pre-exponential factor. In order to determine the value of s accurately, it is necessary to analyze the temperature dependence of the local reduced activation energy $w(T)$ defined as $w(T) = -(1/T)d(\ln\sigma)/d(1/T)$, as was done in Ref. [48]. However, the measurement intervals of $\sigma(T)$ for the p-type 4H-SiC samples are not short enough to calculate $w(T)$.

The Hall factor for NNH in an impurity band can be expressed as [39, 40]

$$A_{ib} = (k_B T/J_3)\exp[K_H(E_3/k_B T)], \quad (2)$$

where J_3 is an adjustable parameter related to the transfer integral (See Eq. (3.5.18) in Ref. [39] and just above Eq. (4) in Ref. [40]). According to Friedman and Holstein [49], the hopping Hall factor activation energy can be expressed as $K_H E_3 = 2E_3 - E'_3$, where E_3 and E'_3 correspond to the two-site and the three-site hopping activation energy, respectively. Friedman and Holstein [49] showed the relation of $E'_3 = (4/3)E_3$for hexagonal crystals. Then, one obtains K_H = 2/3. For cubic crystals,on the

otherhand, K_H has been calculated to between 0 and 2/3 [50]. Ihrig and Hennings [51]showed that K_H= 1/6 for the correlated small polaron hopping. Recently, Avdonin et al. [52] showed that K_H = 1/2 for an equilateral triangle geometry of the hopping sites on the basis of the Feynman's "probability amplitude" approach. In the previous studies of the author, although fitting has been well performed with a constant value of K_H = 2/3 for n-GaAs [53]and n-InP [54],K_H has been found to vary sample to sample for p-type materials of Mn-doped GaAs [47], Mg-doped GaN [33], Mn-doped InSb [34], and InP [35]. In the present study, therefore, K_H has been treated as an adjustable parameter.

Holstein [55] as well as Emin [56] pointed out the possibility of the negative sign of J_3 in spite of hopping in an acceptor impurity band. Holstein [55] claimed that the sign of J_3 for holes, relative to that for electrons, is $-(-1)^n$, where n denotes the number of the hopping sites. For three-site hops, therefore, the sign ofJ_3 for hole hopping is the same as that for electron hopping. Furthermore, Emin [56] showed that the sign of J_3 for both electrons and holesdepends not only on the number of the hopping sitesbut also the nature and the relative orientatins of the local orbitals between which the carrier hops. This leads to the negative sign of J_3 for hopping of holes between s-orbitals in a three-site geometry. According to these studies, J_3 was assume to be negative in the present study.

The Fermi level has been determined by solving the charge-neutrality condition. Tanaka et al. [57] as well as Matsuura et al. [58] took into account the effect of excited states of the acceptor level in the charge-neutrality condition for the analysis on almost non-compensated p-type 4H-SiC with acceptor concentrations less than 10^{19} cm^{-3}.In p-type 4H-SiC samples with acceptor concentrations larger than 10^{19} cm^{-3}, on the other hand, the Coulomb potential originating from an adjacent impurity lowers the potential barrier height for the considered impurity level. This lowering will change the excited states from localized to delocalized to form quasi-continuum [59-62]. This quasi-continuum

state is regarded as part of the valence band. In the present study, therefore, the effect of excited states of the acceptor level was neglected.

The calculation methods of the concentration n_v, the drift mobility μ_v, and the Hall factor A_{Hv} of free holes in the valence band are described in Appendix.

FITTING RESULTS

Contreras et al. [13] prepared p-type 4H-SiC samples by growing epitaxial layers with in-situ Al doping using chemical vapor deposition (CVD)on the Si (0001) face of n-type 4H-SiC substrates. They performed Hall-effect measurements on these samples in the temperature range from 80 to 900 K with varying magnetic fields between −1 and +1 Tesla. Among their samples, Sample S3 exhibited the sign change of the Hall coefficient at 110 K. For this sample, the Al concentration of 7×10^{18} cm^{-3} was measured by secondary ion mass spectroscopy (SIMS) while the net acceptor concentration $N_A - N_D$ of 9.5×10^{18} cm^{-3} was obtained through the electrochemical C-V profiling measurement. Furthermore, Contreras et al. [13] performed thefit to the experimental Hall coefficient using the model described in Ref. [36]. Their obtained values of N_A, N_D, and E_A through the fit areshownin parentheses in the second column of Table I.

Matsuura et al. [18] also prepared two samples of p-type 4H-SiC by growing epitaxial layers using CVD on the Si (0001) face of n-type 4H-SiC substrates: One sample was Al doped (Sample M1) while the other was Al-N codoped (Sample M2). In addition, they prepared an Al-N codoped bulk p-type 4H-SiC sample (Sample M3) by solution growth (SG). The concentrations of Al and N in their samples were measured by SIMS.For Sample M1, the Al concentraion was determined to be 3.4×10^{19} cm^{-3}. The concentrations of Al and N in Sample M2 were determined to be 3.9×10^{19} cm^{-3} and 8.8×10^{18} cm^{-3}, respectively, while those in Sample M3 were determined to be 6.7×10^{19} cm^{-3} and 8.8

× 10^{18} cm^{-3}. They performed Hall-effect measurements on these samples in the temperature range from 60 to 300 K under an AC magnetic field of 0.35 Tesla and 0.05-0.25 Hz. All of three samples exhibited the sign change of the Hall coefficient at low temperatures.

On the other hand, Tone and Zhao [9] prepared five samples (Sample T1 - T5) of p-type 4H-SiC by room-temperature (RT) coimplantation of equal concentrations of C and Al with the concentration range from 1 × 10^{20} to 2 × 10^{21} cm^{-3}. Excepting the sample with the lowest concentration of the implantation, they reported the results of the temperature-dependent Hall-effect measurements on their samples in the temperature range from 130 to 500 K while the data below 170 K are not available for the sample (T1) with the lowest concentration of the implantation provably due to its high resistivity. All the rest four samples show the sign reversal of the Hall coefficient below 170 K.

Fitting to the experimental data on Sample S3 of Ref. [13] (Sample S3), the Al-N codoped CVD-grown sample of Ref. [18] (Sample M2), and five samples of Ref. [9] (Sample T1 - T5)was performed using the model described in the previous section. For Sample T1 of Ref. [9] with the lowest concentration of the implantation, the parameters related to the impurity hopping conduction were not deduced since the data below 170 K are not available. The best-fit values of the fitting parameters are shown in **Table I**.

As can be seen in Table I, the values of N_A, N_D, and E_A obtained for Sample S3 in the present study are almost the same as those obtained in Ref. [13]. In Ref. [13], the values of N_A, N_D, and E_A were obtained through the fit to only the $R_H(T)$ data above 150 K using the temperature-independent value of 2.66 m_0 for the density-of-states (DOS) effective mass m_d, where m_0 is the free-electron mass, together with an analytical expression [36] for the empirical temperature dependence $A_H(T)$ of the Hall factor obtained by Pensl et al. [63]. This method is effective when the logarithmic plot of $n_v(n_v + N_D)/(N_A - N_D - n_v)N_v$ against the reciprocal temperature, where $N_v = 2\left(2\pi m_d k_B T / h^2\right)^{3/2}$ is

the effective DOS of the valence band with h being the Planck constant, approaches a straight line with a slope of $-E_A/k_B$ at high temperatures. This condition was fulfilled for Sample S4 as well as for the Al-N codoped CVD-grown sample. Since the method used in the present study is substantially the same as that used in Ref. [13], it is natural that the values of N_A, N_D, and E_A obtained for Sample S3 in the present study are almost the same as those obtained in Ref. [13].

For Sample T1-T5 in Ref. [9], on the other hand, it is difficult to estimate the values of N_A, N_D, and E_A through the fit to only the $R_H(T)$ data since the logarithmic plot of $n_v(n_v + N_D)/(N_A - N_D - n_v)N_v$ against the reciprocal temperature does not approaches a straight line even at 300 K which is the high end of the measurement temperature range in Ref. [9]. In the present study, however, the simultaneous fits to the $R_H(T)$ and $\sigma(T)$ data enables us to deduce the values of N_A, N_D, and E_A for Sample T1-T5.

Figures 2(a) and 2(b) respectively show the comparison between the experimental and fitted results of the plots of $\sigma T^{3/2}$ and $|R_H|$ as a function of the reciprocal temperature for Sample S3.Solid lines in Fig. 2(a) show the calculated results of $\sigma_{ib}T^{3/2}$ (green) and $\sigma_v T^{3/2}$ (yellow). As can be seen in Fig. 2(a), the transition from hopping conduction to free-hole conduction occurs around 110 K. Figure 2(c) and the inset in Fig. 2(b) respectively show the comparison between the experimental and fitted results of the plots of μ_H and R_H as a function of the temperature. In Fig. 2(b), the calculated results of $(\sigma_v/\sigma)^2 R_{Hv}and(\sigma_{ib}/\sigma)^2 R_{Hib}$ are shown by a green and a yellow curve, respectively. As can be seen in Fig. 2(b), the Hall coefficient reaches its maximum around 110 K at which temperature $\sigma_{ib} = \sigma_v$ is satisfied. On further decreasing temperature, the experimental Hall coefficient decreases tobe 0 and changes its sign to negative. It can be seen in the inset of Fig. 2(b) that the sign change of R_H from positive to negative at around 110 K is owing to the rapid decrease of $(\sigma_v/\sigma)^2 R_{Hv}$ and the rapid increase

of $(\sigma_{ib}/\sigma)^2\left|R_{Hib}\right|$, both of which are caused by the rapid decrease of σ_v/σ_{ib}. It can be seen there that the exponential increase of the absolute value of the negative R_H with decreasing temperature below 100 K is owing to the exponential increase of $\left|R_{Hib}\right|$. It can be seen in Figs. 2(b) and 2(c) that both of $\left|R_H\right|$ and μ_H are well fitted for Sample S3 by including the contribution from the impurity hopping conduction.

Contreras et al. [13] also reported the $R_H(T)$ and $\sigma(T)$ data of Sample S4 for which the Al concentration was determined to be 2×10^{19} cm^{-3} by SIMS. For this sample, their model cannot describe the $R_H(T)$ data with a value of N_A coherent with the Al concentration determined by SIMS: The doping level of more than one order of magnitude would be necessary in the fitting procedure. Their calculation of the mobility also failed to describe the $\mu_H(T)$ data of Sample S4. Such difficulties in fitting to the experimental data of S4 have been confirmed also in the present study.

Figures 3(a) and 3(b) respectively show the comparison between the experimental and fitted results of the plots of $\sigma T^{3/2}$ and $\left|R_H\right|$ as a function of the reciprocal temperature for Sample M2. Solid lines in Fig. 3(a) show the calculated results of $\sigma_{ib}T^{3/2}$ (green) and $\sigma_v T^{3/2}$ (yellow). Figure 3(c) and the inset in Fig. 3(b) respectively show the comparison between the experimental and fitted results of the plots of μ_H and R_H as a function of the temperature. In Fig. 3(b), the calculated results of $(\sigma_v/\sigma)^2 R_{Hv}$ and $(\sigma_{ib}/\sigma)^2 R_{Hib}$ are shown by a green and a yellow curve, respectively. Similar to the case of Sample S3, the transition from hopping conduction to free-hole conduction occurs accompanied by the sign change of the Hall coefficient, but at a much higher temperature around 185 K. It can be seen in Figs. 3(b) and 3(c) that both of $\left|R_H\right|$ and μ_H are well fitted also for Sample M2 by including the contribution from the impurity hopping conduction. This is somewhat astonishing since the Al concentration N_{Al} =

3.9×10^{19} cm^{-3} of this sample determined by SIMS is higher than that of Sample S4 for which our model failed to describe the experimental data well.

For the Al-N codoped SG sample (Sample M3), on the other hand, our model cannot describe the $R_H(T)$ data with a value of N_A coherent with the Al concentration determined by SIMS ($N_{\mathrm{Al}} = 6.7 \times 10^{19}$ cm^{-3}): The doping level of more than twice would be necessary in the fitting procedure. This situation is just like the case of Sample S4 with $N_{\mathrm{Al}} = 2 \times 10^{19}$ cm^{-3}.

Fits to the data were also difficult for the Al-doped sample (Sample M3) grown by CVD. It is known that, besides the bottom Hubbard band formed from the A^0 states (singly occupied acceptor states by holes), the top Hubbard band is formed from the A^+ states (doubly occupied acceptor states by holes) in p-type semiconductors. It is known that NNH conduction in the top Hubbard band, referred as ε_2 conduction, is apt to be important in heavier doped and less compensated samples. For the Al-doped sample, therefore, one may have to consider not only ε_3 conduction in the bottom Hubbard band but also ε_2 conduction in the top Hubbard band.

Figure 4(a) shows the comparison between the experimental and fitted results of the plots of $\sigma T^{3/2}$ as a function of the reciprocal temperature for samples in Ref. [9]. In order to avoid the complexity, the results for only two samples with the implanted Al concentrations of 3×10^{20} cm^{-3} (T2) and 1×10^{21} cm^{-3} (T3) are shown. Open diamonds and closed triangles represent the experimental data of Sample T2 and T3, respectively. Solid lines in Fig. 4(a) show the calculated results of $\sigma_{ib} T^{3/2}$ (green) and $\sigma_v T^{3/2}$ (yellow). The transition from hopping conduction to free-hole conduction can also be seen for these samples.

Figure 4(b) shows the comparison between the experimental and fitted results of the plots of R_H as a function of the temperature for Sample T2 and T3. Solid and dotted lines in Fig. 4(b) show the

calculated results of $(\sigma_v/\sigma)^2 R_{Hv}$ (green) and $(\sigma_{ib}/\sigma)^2 R_{Hib}$ (yellow). The sign reversal occurs at temperatures between 160 and 180 K, which temperatures are higher than for Sample S3 and M2.

DISCUSSION

Activation Ratio of Implanted Al

The problem to be solved in the ion implantation of acceptor impurities to SiC is in low electrical activation ratios of the implanted impurities. In the study of Tone and Zhao [9], the purpose of coimplantation of C ions along with the acceptor dopant Al was to enhance acceptor activation efficiency of Al by intentionally creating a slight imbalance in stoichiometry toward C enrichment, which is expected to enhance the chance for the implanted Al to settle at Si sites. While Tone and Zhao [9] did not estimate the activation ratio (N_A/N_{Al}) of Al for their samples, the activation ratio can now be estimated from the deduced values of the acceptor concentrations N_A in the present study. **Figures 5**(a) and 5(b) respectively show the estimated acceptor concentration N_A and the estimated activation ratio (N_A/N_{Al}) of Al as a function of the implanted Al concentration for the RT C-Al coimplanted samples (T1-T5) annealed at 1500 ºC or 1550 ºC for 30 min in Ref. [9]. It can be seen from Figs. 5(a) and 5(b) that the acceptor concentration saturates at 1×10^{20} cm^{-3}and that the activation ratio decreases from 16 to 4 % when the implanted Al concentration increases from 6×10^{20} to 2×10^{21} cm^{-3}.

Weng et al. [64] annealed their Al implanted samples with the implanted Al concentrations of 1×10^{19} cm^{-3} and 1×10^{20} cm^{-3} at 1650 ºC for 30 min and found that the Al activation ratio is about 10 % for both the Al concentrations. Comparison of the results obtained in the present study for the samples of Ref. [9] with those of Ref. [64] suggests that the C-Al coimplantation has an effect of enhancing the Al activation ratio by a maximum of 1.6 times. This enhancement factor due to coimplantation is consistent with that estimated by Heera et al. [65]. However, the Al activation ratio is still low for the

C-Al coimplanted samples particularly for Al concentrations larger than 1 × 10^{21} cm^{-3}. The low activation ratios may be attributed to clustering of Al into precipitates [65] as was shown by TEM analyses in Ref. [64].

Giannazzo et al. [66] found for their Al implanted 4H-SiC samples with an Al concentration of 1 × 10^{18} cm^{-3} that the Al activation ratio increases from 5 to 75 % when the annealing temperature was increased from 1400 to 1650 ºC. They deduced a value of 16 % as the Al activation ratio for the sample annealed at 1500 ºC for 30 min. The obtained value of 16 % as the Al activation ratio in the present studyfor RT C-Al coimplanted samples annealed at 1500 ºC or 1550 ºCis consistent also with the results of Ref. [66].

The tendency that the Al activation ratio decreases with increasing Al concentration observed in Fig. 5(b) suggests the difficulty of activating Al near its solubility limit (~2 × 10^{20} cm^{-3}) [67] even when coimplanted with C, as pointed out by Rao et al. [68] and Saks et al. [69].

Ionization Energy E_b

In both of Refs. [18] and [9], the acceptor ionization energies E_b were not estimated. In the present study, on the other hand, the simultaneous fits to the experimental data of $\sigma(T)$ and $R_H(T)$ have enabled us to deduce the values of E_b for the samples of Table I. In the previous studies [36, 58, 70-73] on p-type 4H-SiC, the ionization energy of acceptors has been assumed to depend on the total acceptor concentration N_A. Among the studies on p-type 4H-SiC, only Negoro et al. [74] took into account the effect of compensation on the acceptor ionization energy. On the other hand, Tanaka et al. [57] as well as van Daal et al. [75] assumed that the ionization energy of acceptors depend not on the total acceptor concentration N_A but on the ionized acceptor concentration N_A^-, and assumed the relation of $E_b = E_{b0} - \alpha_0 \left(N_A^-\right)^{1/3}$. This is because the Coulomb potential originating from an adjacent

impurity lowers the potential barrier height for the considered impurity level, while that of a neutral impurity is screened by the charge of the trapped carrier. At such low temperatures as $k_B T \ll E_A/\ln[N_v/(2N_A)]$ is satisfied, the approximated relation of $N_A^- \approx N_D$ stands. This is valid below 300 K for p-type 4H-SiC samples with $E_A > 65$ meV. Therefore, the ionization energy of acceptors can be substantially expressed as $E_b = E_{b0} - \alpha_0 N_D^{1/3}$ [75].

In the previous studies of the author on n-type semiconductors of GaAs [53], InP [54], and ZnSe [76], the ionization energies of donor levels have been plotted as a function of the minority impurity (acceptor) concentration. Then, it has been found that the relation of $E_b = E_{b0} - \alpha_0 N_A^{1/3}$ proposed by Pődör [77] shows better fits than the relation of $E_b = E_{b0} - \alpha_0 N_D^{1/3}$ to the experimental results for n-type semiconductors of GaAs [53], InP [54], and ZnSe [76]. The linear dependence of E_b on the cube root of the compensating impurity concentration rather than that of the major impurity concentration has been also shown for p-InP [35].

For n-type GaP and $ZnSiP_2$, Monecke et al. [78] adopted the model in which the ionization energy of donors depends not on the total concentration of donors but on the concentration of ionized donors. Also for p-type materials of 6H-SiC [75], InP [62], GaSb [79], GaN [80], and ZnO [81], it has been found that the ionization energy of acceptors depends not on the total concentration of acceptors but on the concentration of ionized acceptors or that of compensating donors.

In Fig. 6, the values of E_b for the samples of Refs. [13], [18], and [9] listed in Table I deduced in the present study are plotted by a closed circle (●), a triangle (▲), and closed squares (■), respectively, as a function of $N_D^{1/3}$. Also plotted are the E_b data obtained by Pernot et al. [36] (◇), Kasamakova-Kolaklieva et al. [82] (+), Parisini et al. [83] (□), Matsuura et al. [84] (△), Rambach et al. [85] (◆), Nath et al. [86] (*), and Spera et al. [87] (×) for their Al-doped p-type 4H-SiC samples.

A solid straight line indicates the relation assumed by Tanaka et al. [57] which can be expressed as $E_b = E_{b0} - \alpha_0 N_D^{1/3}$, where E_{b0} = 220 meV and α_0= 4.7 ×10^{-5} meV cm. It can be seen in Fig. 6 that the values of E_b deduced for the above samples are almost coincident with this relation.

Activation Energy of ε_3 Conductivity

Matsuura et al. [15] as well as Ji et al. [11] showed that the impurity hopping conduction mechanism is NNH rather than variable-range hopping for the CVD-grown 4H-SiC samples doped with Al concentrations lower than 1.8 × 10^{20} cm^{-3}.Their results are consistent with that in the present study since the concentrations N_A of electrically active Al in all the samples studied in this study have been proved to be lower than 1 × 10^{20} cm^{-3}.

The theoretical expression for the conductivity activation energy ε_3 for NNH has been obtained by [43] as

$$\varepsilon_3 = 0.99 \frac{e^2}{4\pi\varepsilon_0\varepsilon_s} N_A^{1/3}\left(1 - 0.29K^{1/4}\right). \tag{3}$$

Since the hopping conductivity is described by $\sigma_{ib} = e n_{ib} \mu_{ib}$, the activation energy ε_3 of σ_{ib} includes not only the activation energy E_3 of μ_{ib} but also the activation energy of n_{ib}. At sufficiently low temperatures, however, since $n_{ib} = N_A^- N_A^0 / N_A$ can be approximated by the temperature independent value of $n_{ib} \approx N_D (N_A - N_D)/N_A$, the activation energy of n_{ib} can be neglected. Therefore, we can equate ε_3 with E_3.

In Fig. 7, plotted by closed marks are the obtained results of E_3 for the samples listed in Table I while straight lines show the calculated results according to Eq. (3) with ε_s = 9.78: A solid line shows

the result for $K = 0$ while and a broken line shows that for $K = 0.5$. It can be seen there that the plots for the obtained results in the present study are between the two lines.

Ji et al. [11] performed the resistivity (ρ) measurements in the temperature range of 20-900K on their Al-doped samples grown by CVD. The Al concentration N_{Al} in these samples were measured by SIMS to be in the range between 2×10^{19} cm^{-3} and 4×10^{20} cm^{-3}. They found that the Arrhenius plot of ρ shows a distinct change in slope around 100 K. They ascribed the change of the slope to the change of the dominant conduction mechanism from free-hole conduction to NNH conduction. They estimated the activation energy ε_3 of NNH from the slope of the Arrhenius plot of ρ with assuming the temperature-independent pre-exponential factor. The values of $\varepsilon_3$estimated in Ref. [11] are plotted as a function of $N_{\mathrm{Al}}{}^{1/3}$ by open squares in Fig. 7. It can be seen there that the values of ε_3 obtained in Ref. [11] plotted versus $N_{\mathrm{Al}}{}^{1/3}$ are located lower than those of E_3 obtained in the present study plotted versus $N_A{}^{1/3}$. The difference between the values of E_3 obtained in the present study and those of ε_3 obtained by Ji et al. [11] may be partly due to the difference of the temperature dependence of the pre-exponential factor assumed as follows. When assuming the form of Eq. (1) for μ_{ib}, the slope of the Arrhenius plot of σ_{ib} can be written as $d(\ln\sigma_{ib})/d(1/k_BT) \approx -E_3 + (3/2)k_BT$. Therefore, when the value of ε_3 is deduced from the slope of the Arrhenius plot of σ around $T = 100$ K, it will be smaller than the present value of E_3 by $(3/2)k_BT \approx 13$ meV.

Hopping Hall Effect

Very recently, Matsuura et al. [18] proposed a model for explaining the anomalous sign change of the Hall coefficient in their Al-doped p-type 4H-SiC samples. They assumed not only the current I_h due to the hopping of holes from neutral Al (Al^0) sites to their nearest-neighbor negatively ionized Al (Al^-) acceptor sites but also the current I_e due to the hopping of electrons from Al^- sites to their nearest-

neighbor Al^0 sites. When a magnetic field is applied for the Hall-effect measurement, both of hopping holes in I_h and hopping electrons in I_e are forced into the same direction due to the Lorentz force. As the results, the Lorentz force leads to the accumulation of holes and electrons at an electrode. Then, the magnetic field induces not only the Hall voltage V_{Hh} due to the Lorentz force for I_h but also the Hall voltage V_{He} due to the Lorentz force for I_e. Because the existence probabilities of Al^- and Al^0 sites are f_A and $1 - f_A$, respectively, the ratio of the amount of holes to that of electrons accumulated at the electrode is $I_h : I_e = f_A : (1 - f_A)$. Consequently, the ratio between the absolute values of V_{Hh} and V_{He} equals to $f_A : (1 - f_A)$. Since the signs of V_{Hh} and V_{He} are positive and negative, respectively, the total Hall voltage is proportional to $2f_A - 1$. Therefore, Matsuura et al. [18] claimed that the sign of R_{Hib} is positive when $f_A > 0.5$ while negative when $f_A < 0.5$.

This model includes serious flaws. First, it is meaningless to distinguish I_h and I_e. Either of hole hopping from Al^0 to Al^- or electron hopping from Al^- to Al^0 describes the same phenomenon in which charge transfer occurs between Al^- and Al^0. This charge transfer occurs through the quantum-mechanical tunneling process. The Lorenz force is proportional to the velocity of the charged carrier. However, the velocity cannot be defined for this charge transfer process through the quantum-mechanical tunneling. It is therefore impossible to apply the Lorenz force to this charge transfer process.

In addition, whereas some of experimental results, including the results of Matsuura et al. [18], do agree with the prediction that the sign of R_{Hib} is negative when f_A is smaller than 0.5, other experimental results contradict the prediction. At sufficiently low temperature, f_A coincides with the compensation ratio K. Actually, however, it has been demonstrated that R_{Hib} is positive even when K is smaller than 0.5 for several p-type materials, e.g., Cd- or Zn-doped InP [35] and Mn-doped GaAs [47].

Therefore, the sign of R_{Hib} does not have any direct connection to the type of the charge carriers. On the other hand, it is widely accepted now, that the Hall voltage in the hopping regime arises from the quantum interference of the carriers during the hopping motion [88]. In turn, the minimum unit to provide such interference is a triad of closely located sites 1, 2, and 3, so that such triads represent a microscopic structures of the overall Hall effect. Avdonin et al. [52] showed that the difference in phase between the wave function propagating directly from site 1 to site 2 and that propagating from site 1 to site 2 via site 3 is proportional to the magnetic flux Φ through the triangle formed by three sites 1, 2, and 3.

Holstein [55] claimed that the sign of the Hall coefficient for hole hopping is the same as that for electron hoppingwhen the elementary jump-process involves odd members (e.g., three-site hopping) while it is opposite when the elementary jump-process involves even members (e.g., four-site hopping). Emin [56] suggested that the sign of the hopping Hall coefficient depends not only on whether the the elementary jump-process involves even or odd members but also on the symmetry and relative orientation of the local orbitals between which the carrier moves. Kogutyuk et al. [89] as well as Bányai and Aldea [90] suggested that the sign of the hopping Hall coefficient changes as the filling of the impurity band varies, as was assumed by Matsuura et al. [18] but including both of the top and the bottom impurity Hubbard bands. However, none of the above models explain the experimental results well. Furthermore, the value of K_H obtained in the present study varies sample to sample. No tendency can be found against any parameters.

SUMMARY

Simultaneous fits to the experimental data of $\sigma(T)$ and $R_H(T)$ on Al-dopedp-type 4H-SiC have been performed to deduce the impurity concentrations, the acceptor ionization energy, and the

parameters related to the impurity hopping conduction and the hopping Hall effect. The $R_H(T)$ data on Al-doped p-type 4H-SiC reported by Contreras et al. [13] and Matsuura et al. [18] as well as those reported by Tone and Zhao [9] have been well explained within the same model that has been used in the analyses of the data on p-type III-V samples of GaN [33], InSb [34], and InP [35] with the negative Hall factor for the NNH conduction.It has been shown that, being consistent with the small polaron theory in the non-adiabatic case, hopping drift mobility can be described as $\mu_{ib}(T) = \mu_{ib0}\left(\frac{E_3}{k_B T}\right)^{3/2} \exp\left(-\frac{E_3}{k_B T}\right)$, and then the activation energy E_3 has been deduced with taking into account the temperature dependence of the pre-exponential factor. It has also been shown that the anomalous sign reversal of the Hall coefficient to negative can be well explained with assuming the hopping Hall factor in the form of $A_{H3} = (k_B T / J_3)\exp\left(K_H\, E_3 / k_B T\right)$ with the negative sign of J_3.

APPENDIX: Calculation methods for concentration, mobility, and Hall factor of free holes

The concentration n_v of free holes is calculated by $n_v = N_v \cdot \mathcal{F}_{1/2}(\eta)$, where $N_v = 2\left(2\pi m_d k_B T / h^2\right)^{3/2}$ is the effective DOS of the valence band, η is the reduced Fermi level with respect to the edge of the valence band, and $\mathcal{F}_j(\eta)$ is the normalized Fermi-Dirac integral of order j.In the present study, we use the temperature-dependent DOS effective masses, rather than the temperature-independent DOS effective masses, for free holes in p-type 4H-SiC, as in the study by Koizumi et al. [71]. The temperature-dependent DOS effective mass $m_d(T)$ is defined as

$$n_v = 4\pi\left(\frac{2m_d(T)}{h^2}\right)^{3/2} \int_0^\infty f(E,T)E^{1/2}dE\,, \qquad \text{(A1)}$$

where $f(E, T)$ is the Fermi-Dirac distribution function, and has been obtained by Wellenhofer and Rössler [91] for 4H-SiC. We found that the temperature-dependent DOS effective massobtained by

Tanaka et al. [57] can be approximated by$m_d(T)$ = 2.5 m_0/[1 + $(24/T)^{3/4}$] for p-type 4H-SiC in the temperature range between 100 and 900 K.

Tanaka et al. [57] proposed a model for calculating the Hall mobility μ_H and the drift mobility μ_d of p-type 4H-SiC and fitted the calculated results to the experimental data on their almost non-compensated p-type 4H-SiC samples. Their model includes the effects of the anisotropic valence band structure and the anisotropic relaxation times. They showed that the drift mobility μ_d of almost non-compensated p-type 4H-SiC is dominated by acoustic and nonpolar optical phonon scattering at high temperatures while ionized impurity scattering has negligible impact. Furthermore, through the fits to the temperature and acceptor density dependence of mobility, they obtained empirical expressions for the drift mobility and the Hall factor as

$$\mu_d(T, N_A) = \frac{95\mathrm{cm}^2/\mathrm{Vs} \times \left(\frac{T}{300\mathrm{K}}\right)^{-2.1}}{1 + \left(\frac{T}{300\mathrm{K}}\right)^{-1.5}\left(\frac{N_A}{1\times10^{19}\,\mathrm{cm}^{-3}}\right)^{0.71}} \tag{A2}$$

and

$$A_{Hv}(T, N_A) = 1.16 \times \left(\frac{T}{300\mathrm{K}}\right)^{-0.9} \times \frac{1 + \left(\frac{T}{300\mathrm{K}}\right)^{-1.5}\left(\frac{N_A}{1\times10^{19}\,\mathrm{cm}^{-3}}\right)^{0.7}}{1 + \left(\frac{T}{300\mathrm{K}}\right)^{-1.8}\left(\frac{N_A}{3\times10^{18}\,\mathrm{cm}^{-3}}\right)^{0.6}}, \tag{A3}$$

respectively. The former expression agrees with both μ_H/A_H and $\mu_H n_H/n_v$ calculated using their model within about ± 10% error in 200-700K. At lower temperature, however, this expression slightly overestimates the mobility. Furthermore, they suggested that larger errors can arise for higher acceptor concentrations. They also noted that, in case of highly compensated samples, this expression will require some modification to take account of the compensating donor concentration. Such errors at

lower temperatures for higher acceptor concentrations as well as the required modification for the highly compensated case can arise from the effect of ionized impurity scattering.

In the present study, therefore, the effect of impurity scattering is explicitly included in order to calculate the drift mobility μ_v of free holes in moderately compensated heavily doped p-type 4H-SiCat low temperatures. Namely, the drift mobility $\mu_v$is calculated as $1/\mu_v = 1/\mu_{phonon} + 1/\mu_{imp}$, where μ_{phonon} and μ_{imp} denote the lattice-limited and the impurity-limited mobility, respectively. We regard $\mu_d(T, 0)$ as μ_{phonon}. The impurity-limited mobility is calculated as $1/\mu_{imp} = 1/\mu_{ii} + 1/\mu_{ni}$, where μ_{ii} and μ_{ni} denote the mobility due to ionized-impurity scattering and that due to neutral-impurity scattering, respectively.

Tanaka et al. [57] calculated conductivity tensors and the drift mobility on the basis of the relaxation-time approximation. In Ref. [57], the relaxation time τ_{ii} due to ionized-impurity scattering was calculated using the Brooks-Herring formula. Then, Tanaka et al. [57] multiplied the relaxation time τ_{ii} by a factor of 2 in order to take into account the p-type symmetry of wave functions in place of the s-type wave functions while Pernot et al. [36] as well as Koizumi et al. [71] multiplied it by a factor of 3/2. However, Poklonski et al. showed that the Brooks-Herring formula gives an overestimated value of the mobility (and thus the relaxation time τ_{ii}) for p-type Si [92] as well as for n-type InSb [93] even when the value is not multiplied. When using the Brooks-Herring formulafor the calculation of hole mobility, Lowney and Bennett [94] preferred not to multiply τ_{ii} by the overlap factor because of the relative strength of small-angle scattering and the fact that the overlap factor due to the p-wave nature of holes goes to unity for small angles. In the present study, therefore, the relaxation time τ_{ii} due to ionized impurity scattering has been calculated using the Brooks-Herring formula without any multiplication as in the previous studies of the author on p-type materials [35, 47].

On the other hand, for the calculation of τ_{ii}, we have taken into account the effect of the increase of the static dielectric constant at the insulator side of the MI transition. It has been shown both experimentally and theoretically that the static dielectric constant at low temperature increases with the impurity concentration to diverge at the critical net acceptor concentration N_{NAcr} for the onset of the MI transition [95, 96]. According to Poklonski et al. [96], we assume the form of

$$\varepsilon_{eff}(N_A^0) = \left(\varepsilon_s + 2N_A^0/N_{NAcr}\right)\left(1 - N_A^0/N_{NAcr}\right)^{-1}. \quad \text{(A4)}$$

Regarding the critical concentration for the MI transition in Al-doped p-type 4H-SiC, we adopt the value of N_{NAcr} = 2.1 × 10^{20} cm^{-3}according to Persson et al. [97], and calculated ε_{eff} according to Eq. (A4).

In the calculation of the energy-dependent relaxation time $\tau_{ii}(E)$ due to ionized-impurity scattering, Tanaka et al. [57] as well as Koizumi et al. [71] and Parisini et al. [83] took into account not only screening due to free holes but also that due to hopping carriers [98] for calculating the inverse screening length β_s (Note that there are nontrivial errors related to the Fermi-Dirac integral in Eq. (A2) for β_s in Ref. [83]). In the present study, however, only screening due to free holes has been taken into account for calculating $\tau_{ii}(E)$ of free holeswithout the effect of hopping carriers. In order to calculate the drift mobility, it is necessary to average $\tau_{ii}(E)$ by integral of E. The Brooks-Herring formula for $\tau_{ii}(E)$ contains a factor $B_{ii}(b) = \ln(b+1) - b/(b+1)$, where $b = 8m_d E/(\hbar\beta_s)^2$. Although the factor $B_{ii}(b)$ is a function of E, its dependence is slow. Owing to this, $B_{ii}(b)$ can be replaced before the integral of EdE by a constant value of $B_{ii}(b_{max})$, where b_{max} represents the value of b at which the integral becomes the maximum. One can calculate b_{max} as [99]

$$b_{max} = \frac{4\pi\varepsilon_{eff}(k_B T)^{1/2}h}{e^2(2m_d)^{1/2}}\frac{5}{\sqrt{\pi}}\cdot\mathcal{F}_{3/2}(\eta)/[\cdot\mathcal{F}_{-1/2}(\eta)\cdot\mathcal{F}_{1/2}(\eta)]. \quad \text{(A5)}$$

Then, the drift mobility due to ionized impurity scattering can be calculated as

$$\mu_{ii} = \frac{(4\pi\varepsilon_{eff})^2 (k_B T)^{3/2}}{N_{ii}\pi e^3 (2m_d)^{1/2} B_{ii}(b_{max})} 2\mathcal{F}_2(\eta)/\mathcal{F}_{1/2}(\eta). \quad \text{(A6)}$$

The calculation of μ_{ni} have been performed according to Erginsoy's model. Namely, it is calculated as

$$\mu_{ni} = \frac{e}{20 a_B \hbar} \frac{m^*/m_0}{4\pi\varepsilon_{eff}\varepsilon_0 N_A^0}, \quad \text{(A7)}$$

where $a_B = 4\pi\varepsilon_{eff}\varepsilon_0\hbar^2 / m^* e^2$ is the Bohr radius describing the bound hole at the neutral acceptor. Tanaka et al. [57] treated the hole effective mass in Eq. (A7) as an adjustable parameter which is irrespective of the DOS and the conductivity effective masses to assume it to be 1.0 × m_0 to reproduce the experimental mobility at low temperatures and high concentrations of acceptors in p-type 4H-SiC. In the present study, the hole effective mass for the calculation using Eq. (A7) was also assumed to be 1.0 × m_0.

CONFLICT OF INTEREST

The author declares that there is no conflict of interest.

REFERENCES

[1] G. Buch and H. Labhart, Helv. Phys. Acta. 19, 463 (1946).
[2] C. S. Hung and J. R. Gliessman, Phys. Rev. 79, 726 (1950).
[3] G. A. Lomakina, E. N. Mokhov and V. G. Oding, Sov. Phys. Semicond. 17, 72 (1983).
[4] H. J. van Daal, Philips Res. Rep. Suppl. 3, 1 (1965).
[5] M. N. Alexander, Phys. Rev. 172, 331 (1968).
[6] M. V. Alekseenko, A. I. Veinger, A. G. Zabrodskii, V. A. Ilin, Y. M. Tairov and V. F. Tsvetkov, JETP Lett. 39, 304 (1984).
[7] A. O. Evwaraye, S. R. Smith, W. C. Mitchel and M. D. Roth, Appl. Phys. Lett. 68, 3159 (1996).
[8] W. C. Mitchel, A. O. Evwaraye, S. R. Smith and M. D. Roth, J. Electron. Mater. 26, 113 (1997).

[9] K. Tone and J. H. Zhao, IEEE Trans. Electron Devices 46, 612 (1999).
[10] V. Heera, K. N. Madhusoodanan, W. Skorupa, C. Dubois and H. Romanus, J. Appl. Phys. 99, 123716 (2006).
[11] S. Ji, K. Eto, S. Yoshida, K. Kojima, Y. Ishida, S. Saito, H. Tsuchida and H. Okumura, Appl. Phys. Express 8, 121302 (2015).
[12] A. Parisini, M. Gorni, A. Nath, L. Belsito, M. V. Rao and R. Nipoti, J. Appl. Phys. 118, 035101 (2015).
[13] S. Contreras, L. Konczewicz, P. Kwasnicki, R. Arvinte, H. Peyre, T. Chassagne, M. Zielinski, M. Kayambaki, S. Juillaguet and K. Zekentes, Mater. Sci. Forum 858, 249 (2016).
[14] A. Parisini and R. Nipoti, J. Phys.-Condensed Matter 29, 035703 (2017).
[15] H. Matsuura, A. Takeshita, T. Imamura, K. Takano, K. Okuda, A. Hidaka, S. Y. Ji, K. Eto, K. Kojima, T. Kato, S. Yoshida and H. Okumura, Mater. Sci. Forum 924, 188 (2018).
[16] H. Matsuura, A. Takeshita, T. Imamura, K. Takano, K. Okuda, A. Hidaka, S. Y. Ji, K. Eto, K. Kojima, T. Kato, S. Yoshida and H. Okumura, Appl. Phys. Express 11, 101302 (2018).
[17] H. Matsuura, A. Takeshita, T. Imamura, K. Takano, K. Okuda, A. Hidaka, S. Ji, K. Eto, K. Kojima, T. Kato, S. Yoshida and H. Okumura, Jpn. J. Appl. Phys. 58, 098004 (2019).
[18] H. Matsuura, A. Takeshita, A. Hidaka, S. Y. Ji, K. Eto, T. Mitani, K. Kojima, T. Kato, S. Yoshida and H. Okumura, Jpn. J. Appl. Phys. 59, 051004 (2020).
[19] M. Krieger, K. Semmelroth and G. Pensl, Mater. Sci. Forum 457-460, 685 (2004).
[20] H. Yonemitsu, H. Maeda and H. Miyazawa, J. Phys. Soc. Jpn. 15, 1717 (1960).
[21] A. B. Henriques, N. F. Oliveira Jr., S. A. Obukhov and V. A. Sanina, JETP Lett. 69, 386 (1999).
[22] S. A. Obukhov, Solid State Commun. 70, 103 (1989).
[23] S. A. Obukhov, Phys. Stat. Sol. B 242, 1298 (2005).
[24] S. A. Obukhov, Phys. Stat. Sol. C 9, 247 (2012).
[25] S. A. Obukhov, S. W. Tozer and W. A. Coniglio, Sci. Rep. 5, 13451 (2015).
[26] D. L. Partin, J. Heremans and C. M. Thrush, J. Cryst. Growth 175/176, 860 (1997).
[27] M. Benzaquen, B. Belache and C. Blaauw, Phys. Rev. B 46, 6732 (1992).
[28] M. Benzaquen, B. Belache and D. Walsh, Phys. Rev. B 44, 13105 (1991).
[29] S. B. Mikhirin and K. F. Shtel'makh, Physica B 308-310, 881 (2001).
[30] B. Gunning, J. Lowder, M. Moseley and W. A. Doolittle, Appl. Phys. Lett. 101, 082106 (2012).
[31] M. Jaime, H. T. Hardner, M. B. Salamon, M. Rubinstein, P. Dorsey and D. Emin, Phys. Rev. Lett. 78, 951 (1997).
[32] N. V. Agrinskaya, V. I. Kozub and D. S. Poloskin, Semicond. 44, 472 (2010).
[33] Y. Kajikawa, Phys. Stat. Sol. C 14, 1600129 (2017).
[34] Y. Kajikawa, Phys. Stat. Sol. C 14, 1600215 (2017).
[35] Y. Kajikawa, Phys. Stat. Sol. C 14, 1600217 (2017).
[36] J. Pernot, S. Contreras and J. Camassel, J. Appl. Phys. 98, 023706 (2005).
[37] N. A. Poklonski and V. F. Stelmakh, Phys. Stat. Sol. B 117, 93 (1983).
[38] N. A. Poklonskiĭ and S. Y. Lopatin, Phys. Solid State 43, 2219 (2001).
[39] H. Böttger and V. V. Bryksin, Hopping Conduction in Solids, (Akademie-Verlag, Berlin, 1985).
[40] P. Nagels in The Hall Effect and Its Applications, ed. By C. L. Chien and C. R. Westgate, (Plenum, New York, 1980), p. 253.

[41] T. Holstein, Ann. Phys. 8, 343 (1959).
[42] T. Holstein, Ann. Phys. 281, 725 (2000).
[43] B. I. Shklovskii and A. L. Efros, Electronic Properties of Doped Semiconductors, (Springer-Verlag, Berlin, 1984).
[44] R. Mansfield, S. Abboudy and P. Fozooni, Phil. Mag. B 57, 777 (1988).
[45] N. A. Poklonski, S. A. Vyrko, O. N. Poklonskaya and A. G. Zabrodskii, J. Appl. Phys. 110, 123702 (2011).
[46] N. A. Poklonski, S. A. Vyrko, O. N. Poklonskaya, A. I. Kovalev and A. G. Zabrodskii, J. Appl. Phys. 119, 245701 (2016).
[47] Y. Kajikawa, Phys. Stat. Sol. C 13, 387 (2016).
[48] Y. Kajikawa, Int. J. Mod. Phys. B 34, 2050069 (2020).
[49] L. Friedman and T. Holstein, Ann. Phys. 21, 494 (1963).
[50] V. V. Bryskin and Y. A. Firsov, Sov. Phys. Solid State 12, 480 (1970).
[51] H. Ihrig and D. Hennings, Phys. Rev. B 17, 4593 (1978).
[52] A. Avdonin, P. Skupinski and K. Graza, Physica B 483, 13 (2016).
[53] Y. Kajikawa, Phys. Stat. Sol. B 255, 1800063 (2018).
[54] Y. Kajikawa, Phys. Stat. Sol. B 257, 1900354 (2019).
[55] T. Holstein, Phil. Mag. 27, 225 (1973).
[56] D. Emin, Phil. Mag. 35, 1189 (1977): D. Emin, in The Hall Effect and Its Applications, ed. By C. L. Chien and C. R. Westgate, (Plenum, New York,1980), p. 281.
[57] H. Tanaka, S. Asada, T. Kimoto and J. Suda, J. Appl. Phys. 123, 245704 (2018).
[58] H. Matsuura, M. Komeda, S. Kagamihara, H. Iwata, R. Ishihara, T. Hatakeyama, T. Watanabe, K. Kojima, T. Shinohe and K. Arai, J. Appl. Phys. 96, 2708 (2004).
[59] K. C. Shifrin, J. Phys. U.S.S.R. 8, 242 (1944).
[60] G. E. Stillman and C. M. Wolfe, Thin Solid Films 31, 69 (1976).
[61] J. S. Blakemore, Semiconductor Statistics, (Dover, Mineola, 1987).
[62] K. Hansen, E. Peiner, A. Schlachetzki and M. Vonortenberg, J. Electron. Mater. 23, 935 (1994).
[63] G. Pensl, F. Schmid, F. Ciobanu, M. Laube, S. A. Reshanov, N. Schulze, K. Semmelroth, H. Nagasawa, A. Schoner and G. Wagner, Mater. Sci. Forum 433-436, 365 (2002).
[64] M. H. Weng, F. Roccaforte, F. Giannazzo, S. Di Franco, C. Bongiorno, M. Saggio and V. Raineri, Mater. Sci. Forum 645-648, 713 (2010).
[65] V. Heera, D. Panknin and W. Skorupa, Appl. Surf. Sci. 184, 307 (2001).
[66] F. Giannazzo, F. Roccaforte and V. Raineri, Appl. Phys. Lett. 91, 202104 (2007).
[67] M. K. Linnarsson, M. S. Janson, U. Zimmermann, B. G. Svensson, P. O. A. Persson, L. Hultman, J. Wong-Leung, S. Karlsson, A. Schoner, H. Bleichner and E. Olsson, Appl. Phys. Lett. 79, 2016 (2001).
[68] M. V. Rao, J. B. Tucker, M. C. Ridgway, O. W. Holland, N. Papanicolaou and J. Mittereder, J. Appl. Phys. 86, 752 (1999).
[69] N. S. Saks, A. V. Suvorov and D. C. Capell, Appl. Phys. Lett. 84, 5195 (2004).
[70] P. Achatz, J. Pernot, C. Marcenat, J. Kacmarcik, G. Ferro and E. Bustarret, Appl. Phys. Lett. 92, 072103 (2008).
[71] A. Koizumi, J. Suda and T. Kimoto, J. Appl. Phys. 106, 013716 (2009).
[72] S. Contreras, L. Konczewicz, R. Arvinte, H. Peyre, T. Chassagne, M. Zielinski and S. Juillaguet, Phys. Stat. Sol. A 214, 1600679 (2017).
[73] C. Darmody and N. Goldsman, J. Appl. Phys. 126, 145701 (2019).

[74] Y. Negoro, T. Kimoto, H. Matsunami, F. Schmid and G. Pensl, J. Appl. Phys. 96, 4916 (2004).
[75] H. J. van Daal, W. F. Knippenberg and J. D. Wasscher, J. Phys. Chem. Solids 24, 109 (1963).
[76] Y. Kajikawa, Phil. Mag. 100, 2018 (2020).
[77] B. Pődör, Semicond. Sci. Technol. 2, 177 (1987).
[78] J. Monecke, W. Siegel, E. Ziegler and G. Kühnel, Phys. Stat. Sol. B 103, 269 (1981).
[79] F. Meinardi, A. Parisini and L. Tarricone, Semicond. Sci. Technol. 8, 1985 (1993).
[80] W. Gotz, R. S. Kern, C. H. Chen, H. Liu, D. A. Steigerwald and R. M. Fletcher, Mater. Sci. Eng. B 59, 211 (1999).
[81] O. Lopatiuk-Tirpak, W. V. Schoenfeld, L. Chernyak, F. X. Xiu, J. L. Liu, S. Jang, F. Ren, S. J. Pearton, A. Osinsky and P. Chow, Appl. Phys. Lett. 88, 202110 (2006).
[82] L. Kasamakova-Kolaklieva, L. Storasta, I. G. Ivanov, B. Magnusson, S. Contreras, C. Consejo, J. Pernot, M. Zielinski and E. Janzen, Mater. Sci. Forum 457-460, 677 (2004).
[83] A. Parisini and R. Nipoti, J. Appl. Phys. 114, 243703 (2013).
[84] H. Matsuura, K. Sugiyama, K. Nishikawa, T. Nagata and N. Fukunaga, J. Appl. Phys. 94, 2234 (2003).
[85] M. Rambach, A. J. Bauer and H. Ryssel, Phys. Stat. Sol. B 245, 1315 (2008).
[86] A. Nath, R. Scaburri, M. V. Rao and R. Nipoti, Mater. Sci. Forum 717-720, 237 (2012).
[87] M. Spera, D. Corso, S. Di Franco, G. Greco, A. Severino, P. Fiorenza, F. Giannazzo and F. Roccaforte, Mater. Sci. Semicond. Processing 93, 274 (2019).
[88] T. Holstein, Phys. Rev. 124, 1329 (1961).
[89] I. P. Kogutyuk, V. M. Nitsoich and F. V. Skrypnik, Phys. Stat. Sol. B 99, 183 (1980).
[90] L. Bányai and A. Aldea, Phys. Rev. 143, 652 (1966).
[91] G. Wellenhofer and U. Rössler, Phys. Stat. Sol. B 202, 107 (1997).
[92] N. A. Poklonski, A. V. Denisenko, S. Y. Lopatin and A. I. Siaglo, Phys. Stat. Sol. B 206, 713 (1998).
[93] N. A. Poklonski, S. A. Vyrko, V. I. Yatskevich and A. A. Kocherzhenko, J. Appl. Phys. 93, 9749 (2003).
[94] J. R. Lowney and H. S. Bennett, J. Appl. Phys. 69, 7102 (1991).
[95] S. Abboudy, Int. J. Mod. Phys. B 10, 59 (1996).
[96] N. A. Poklonski, S. A. Vyrko and A. G. Zabrodskii, Phys. Solid State 46, 1101 (2004).
[97] C. Persson, A. F. da Silva and B. Johansson, Phys. Rev. B 63, 205119 (2001).
[98] T. N. Morgan, Phys. Rev. 139, A343 (1965).
[99] Y. Kajikawa, J. Appl. Phys. 114, 043719 (2013).

Table I. Values used for fitting to the experimental data on Sample S3 of Refs. [13], Sample M2 of Ref. [18], and Sample T1 - T5 of Ref. [9].The values in parentheses in the second column are those obtained through the fit in Ref. [13] while the values in brackets in the third column are those obtained through the SIMS measurements in Ref. [18].

Sample	S3	M2	T1	T2	T3	T4	T5
N_{Al} (10^{19} cm^{-3})	0.7	3.9	10	30	60	100	200
N_A (10^{19} cm^{-3})	1.0 (1.0)	1.35	0.9	3.9	9.6	8.6	7.6
N_D (10^{19} cm^{-3})	0.001 (0.001)	0.5 [0.88]	0.5	1.8	2.1	2.9	3.0
$K = N_D/N_A$	0.001 (0.001)	0.37 [0.23]	0.56	0.46	0.22	0.34	0.39
E_A (meV)	186 (190)	93	98	72	101	81	74
E_3 (meV)	34	30		52	55	59	59
μ_{ib0} (cm^2/Vs)	0.8	0.2		1.6	2.6	2.2	1.9
K_H	1.8	0.55		0.95	1.4	1.0	1.0
J_3 (meV)	-33	-40		-1200	-22000	-3500	-3000

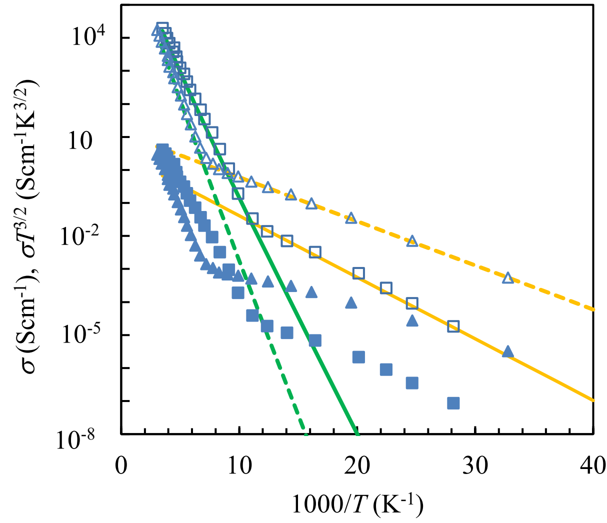

Fig. 1. Arrhenius plots of σ (closed markes) and $\sigma T^{3/2}$ (open markes) for the samples of p-type 4H-SiC reported by Matsuura et al. [15]: Squares and triangles respectively represent the experimental results for the Al-doped sample with the Al concentration of 2.4×10^{19} cm^{-3} and for the Al-N codoped sample with the concentrations of Al and N of 1.4×10^{19} cm^{-3} and 7.0×10^{18} cm^{-3}. The solid and broken lines indicate the band and NNH conductions at higher and lower temperatures, respectively.

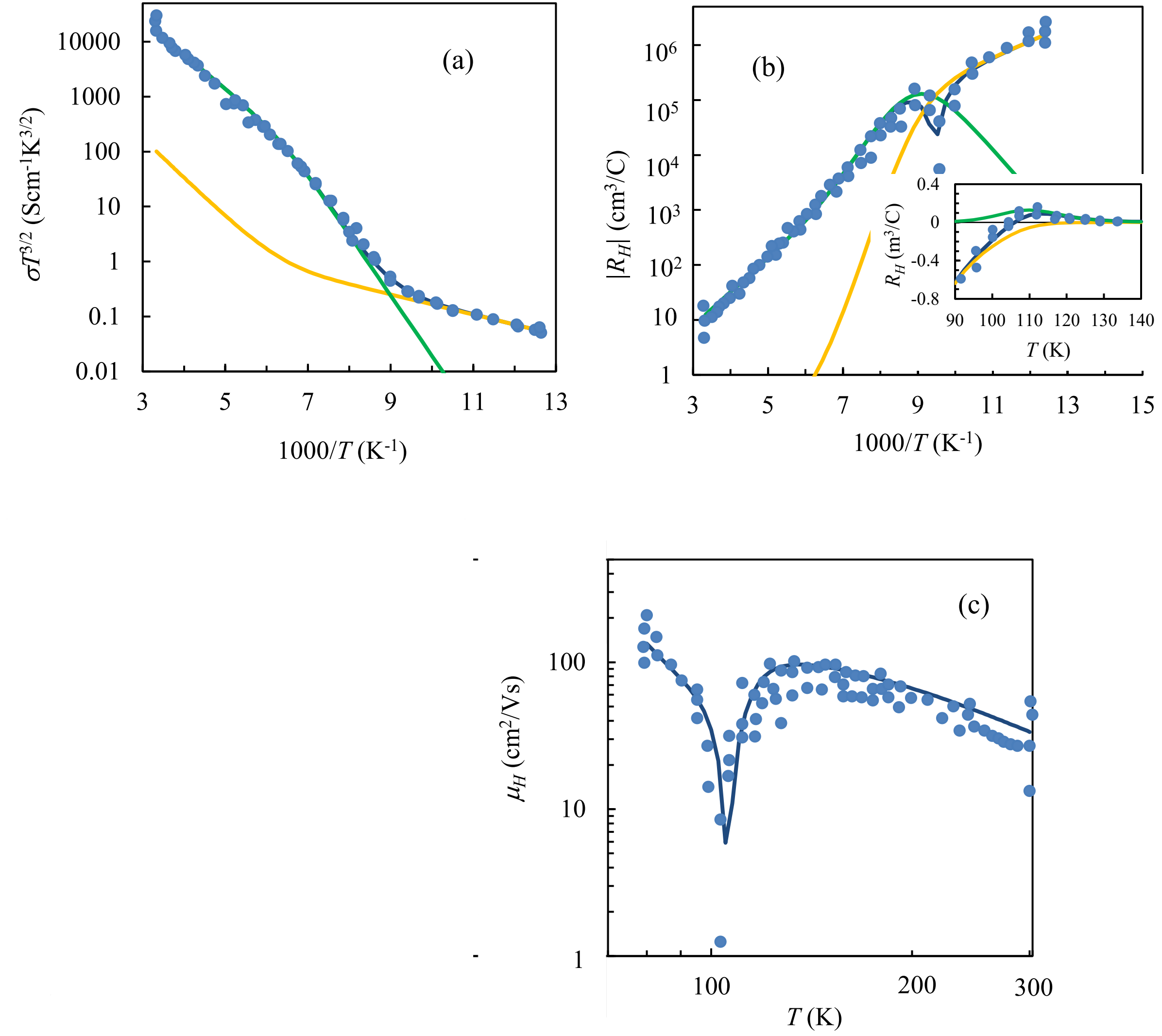

Fig. 2. Comparison between the experimental and fitted results for Sample S3 of Al-doped p-type 4H-SiC reported by Contreras et al. [13]: (a) the plot of $\sigma T^{3/2}$ as a function of the reciprocal temperature; (b) the plot of $|R_H|$ as a function of the reciprocal temperature; (c) the plot of μ_H as a function of the temperature. The inset in (b) shows the plot of R_H as a function of the temperature. Green and yellow curves represent the calculated results of the contributions from free-hole conduction and impurity hopping conduction, respectively.

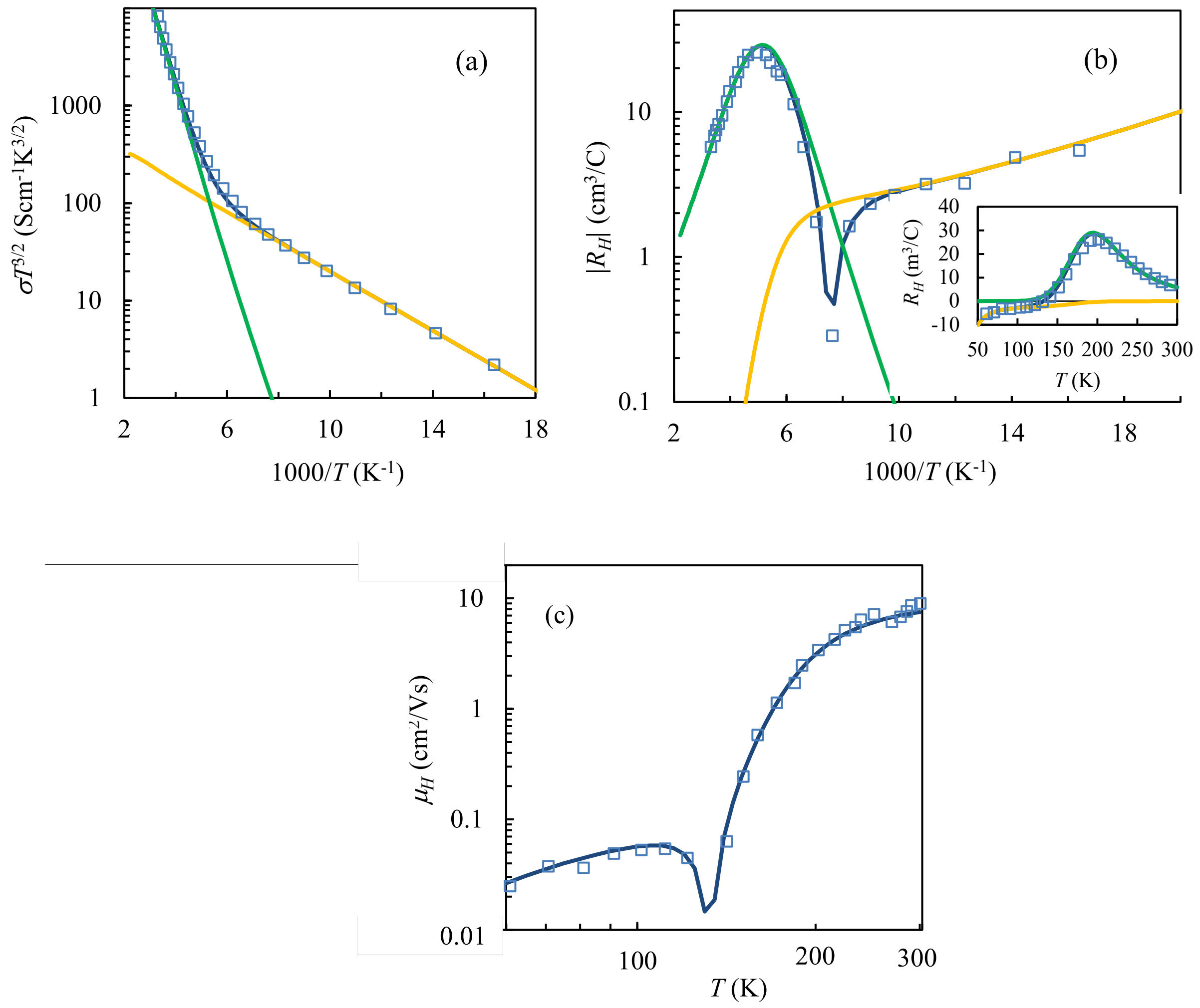

Fig. 3. The same as Fig. 2 but for the Al-N codoped sample (Sample M2) grown by CVD of Ref. [18].

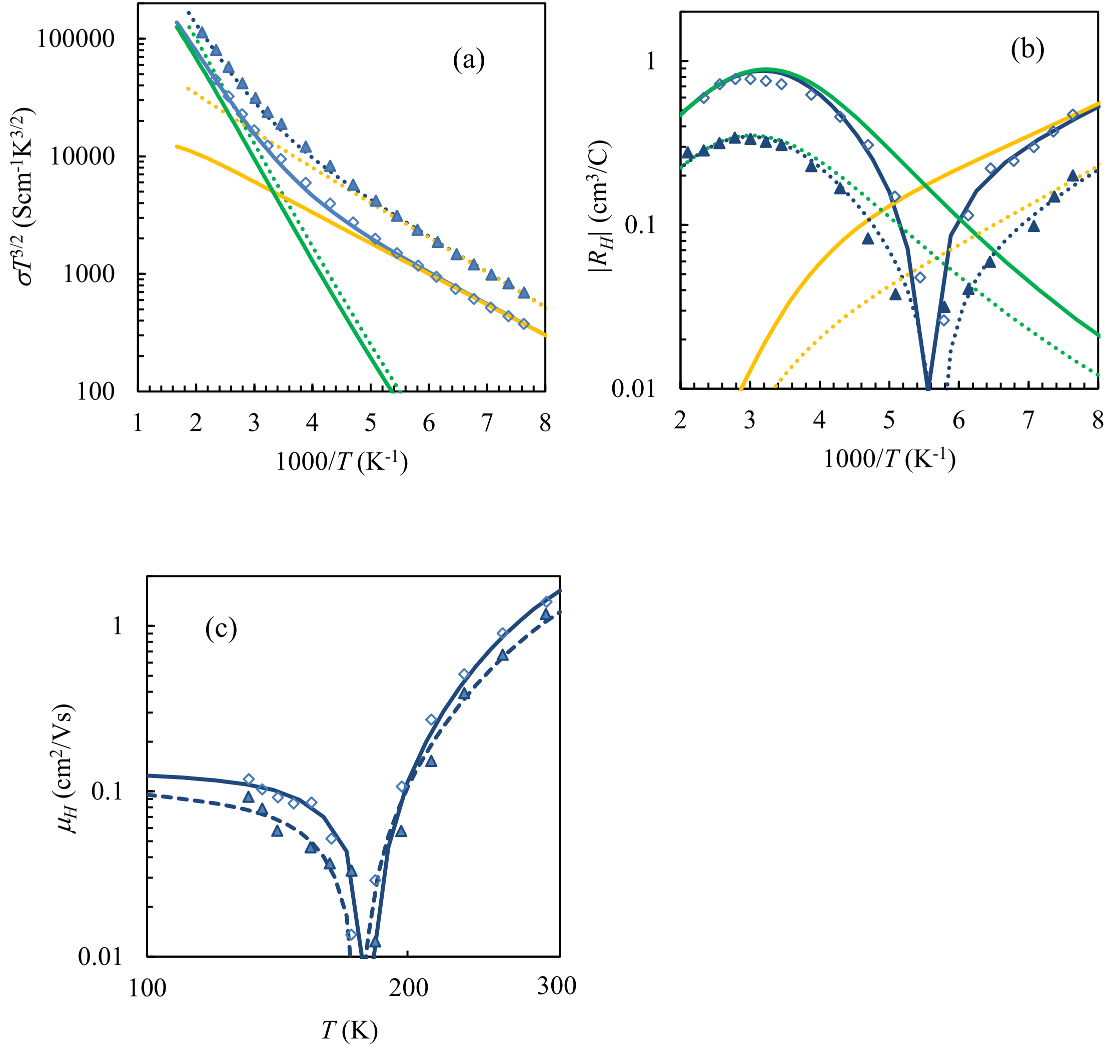

Fig. 4. Comparison of between the experimental and fitted results for the two samples of RT C plus Al coimplanted p-type 4H-SiC of Ref. [9]: (a) the plot of $\sigma T^{3/2}$as a function of the reciprocal temperature; (b) the plot of $|R_H|$ as a function of the reciprocal temperature; (c) the plot of μ_H as a function of the temperature. Open diamonds and closed triangles represent the experimental results for the samples implanted with Al concentrations of 3 × 10^{20} cm^{-3} (Sample T2) and 1 × 10^{21} cm^{-3} (Sample T3), respectively, while solid and dotted curves represent the calculated results for the former and the latter samples, respectively.

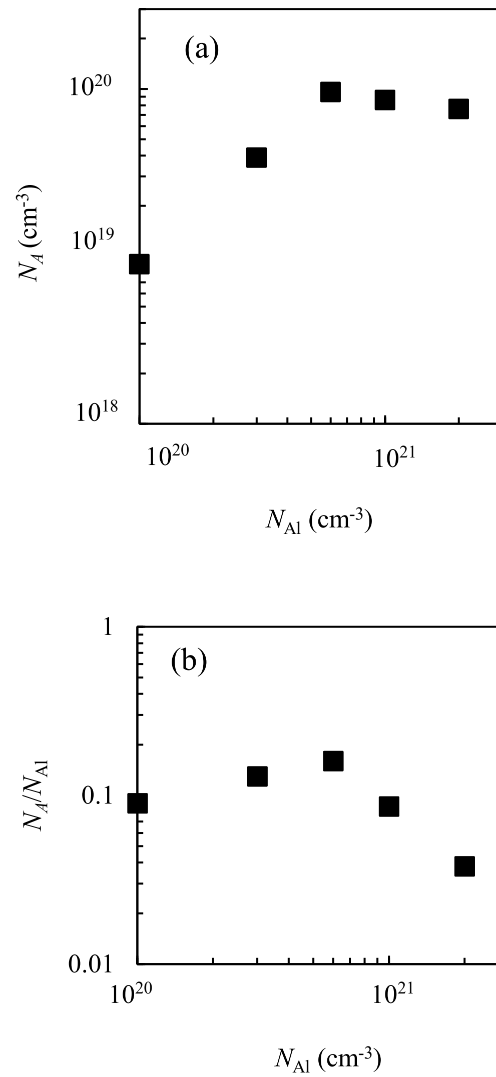

Fig. 5 (a) Acceptor concentration N_A and (b) Al activation ratio N_A/N_{Al} as a function of the implanted Al concentration N_{Al} for the RT C-Al coimplanted samples (T1-T5) of Ref. [9].

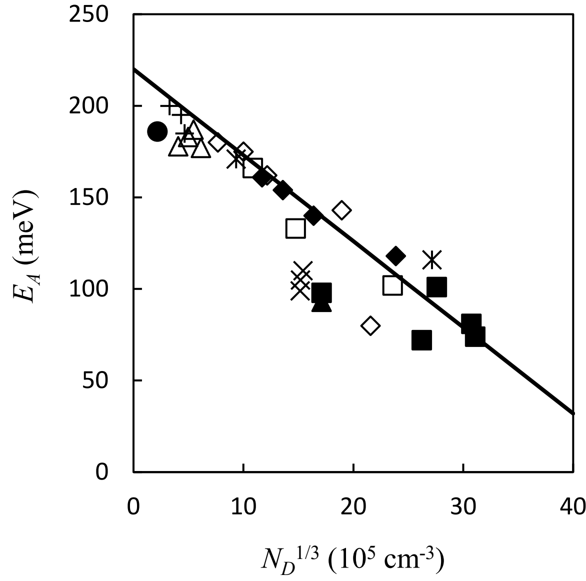

Fig. 6 The plot of E_A as a function of $N_D^{1/3}$. A closed circle (●), a closed triangle (▲), and closed squares (■)respectively represent the results obtained in the present study for samples of Refs. [13], [18] and [9] listed in Table I. Also shown are the results obtained by Matsuura et al. [84] (△), Kasamakova-Kolaklieva et al. [82] (+), Pernot et al. [36] (◇), Rambach et al. [85] (◆), Parisini et al. [83] (□), Nath et al. [86] (*), and Spera et al. [87] (×). A solid line represents the relation of $E_b = E_{b0} - \alpha_0 N_D^{1/3}$, where E_{b0} = 220 meV and $\alpha_0 = 4.7 \times 10^{-5}$ meV cm, which was assumed by Tanaka et al. [57].

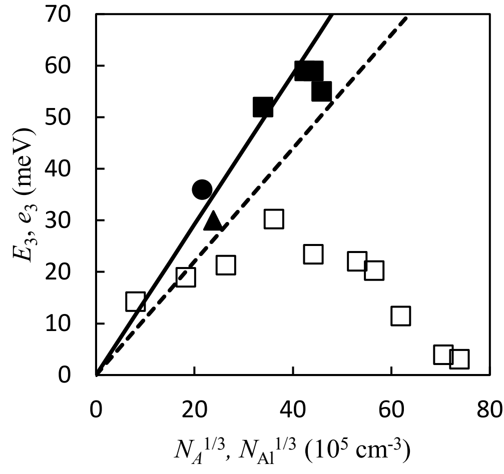

Fig. 7. The plot of E_3 as a function of $N_A^{1/3}$: Closed marks of a circle, a triangle, and squares respectively represent the results for the samples of Refs. [13], [18], and [9] listed in Table I. A solid and a broken line represent the relations of Eq. (3) with $K = 0$ and 0.5, respectively. Open squares show the plot of ε_3 as a function of $N_{Al}^{1/3}$ reported in Ref. [11].